

Time-resolved thermal mirror technique with top-hat cw laser excitation

Francine B. G. Astrath,¹ Nelson G. C. Astrath,^{1,*} Jun Shen,^{1,**} Jianqin Zhou,¹ Luis C. Malacarne,² P. R. B. Pedreira,² and Mauro L. Baesso²

¹ National Research Council of Canada, Institute for Fuel Cell Innovation, 4250 Wesbrook Mall, Vancouver, British Columbia V6T 1W5, Canada

² Departamento de Física, Universidade Estadual de Maringá, Avenida Colombo 5790, 87020-900, Maringá, Paraná, Brasil

*E-mail address: AstrathNGC@pq.cnpq.br; **Corresponding author: Jun.Shen@nrc-cnrc.gc.ca

Abstract: A theoretical model was developed for time-resolved thermal mirror spectroscopy under top-hat cw laser excitation that induced a nanoscale surface displacement of a low absorption sample. An additional phase shift to the electrical field of a TEM₀₀ probe beam reflected from the surface displacement was derived, and Fresnel diffraction theory was used to calculate the propagation of the probe beam. With the theory, optical and thermal properties of three glasses were measured, and found to be consistent with literature values. With a top-hat excitation, an experimental apparatus was developed for either a single thermal mirror or a single thermal lens measurement. Furthermore, the apparatus was used for concurrent measurements of thermal mirror and thermal lens. More physical properties could be measured using the concurrent measurements.

©2008 Optical Society of America

OCIS codes: (300.6430) Photothermal Spectroscopy; (160.6840) Thermo-optical materials

References and links

1. M. A. Olmstead, N. M. Amer, S. Kohn, D. Fournier, and A. C. Boccara, "Photothermal displacement spectroscopy - an optical probe for solids and surfaces," *Appl. Phys. A* **32**, 141-154 (1983).
2. D. P. Almond and P. M. Patel, *Photothermal Science and Techniques* (Chapman and Hall, London, 1996).
3. R. D. Snook and R. D. Lowe, "Thermal lens spectrometry. A review," *Analyst* **120**, 2051-2068 (1995)
4. S. E. Bialkowski, "*Photothermal Spectroscopy Methods for Chemical Analysis*" (Wiley, New York, 1996).
5. M. L. Baesso, J. Shen, and R. D. Snook, "Mode-mismatched thermal lens determination of temperature coefficient of optical path length in soda lime glass at different wavelengths," *J. Appl. Phys.* **75**, 3732-3737 (1994).
6. Y. S. Lu, P. K. Kuo, L. D. Favro, R. L. Thomas, Z. L. Wu, and S. T. Gu, "Diffraction patterns of a surface thermal lens," *Progr. Natural Sci.* **6**, S202-S205 (1996).
7. B. C. Li, "3-Dimensional theory of pulsed photothermal deformation," *J. Appl. Phys.* **68**, 482-487 (1990).
8. N. G. C. Astrath, L. C. Malacarne, P. R. B. Pedreira, A. C. Bento, M. L. Baesso, and J. Shen, "Time-resolved thermal mirror for the measurements of thermo-optical-mechanical properties of low absorbing solids," *Appl. Phys. Lett.* **91**, 191908/1-191908/3 (2007).
9. L. C. Malacarne, F. Sato, P. R. B. Pedreira, A. C. Bento, R. S. Mendes, M. L. Baesso, N. G. C. Astrath, and J. Shen, "Nanoscale surface displacement detection in high absorbing solids by time-resolved thermal mirror," *Appl. Phys. Lett.* **92**, 131903/1 - 131903/3 (2008).
10. B. C. Li, S. Xiong and Y. Zhang, "Fresnel diffraction model for mode-mismatched thermal lens with top-hat beam excitation," *Appl. Phys. B* **80**, 527-534 (2005).
11. N. G. C. Astrath, F. B. G. Astrath, J. Shen, J. Zhou, P. R. B. Pedreira, L. C. Malacarne, A. C. Bento, and M. L. Baesso "Top-hat cw-laser-induced time-resolved mode-mismatched thermal lens spectroscopy for quantitative analysis of low absorption materials," *Opt. Lett.* **33**, 1464-1466 (2008).
12. H. S. Carslaw and J. C. Jaeger, *Conduction of heat in solids* (Clarendon Press, Oxford, 1959).
13. W. Nowacki, *Thermoelasticity* (Pergamon, Oxford, 1982).
14. F. Sato, L. C. Malacarne, P. R. B. Pedreira, M. P. Belancon, R. S. Mendes, M. L. Baesso, N. G. C. Astrath, and J. Shen, "Time-resolved thermal mirror method: A theoretical study," *J. Appl. Phys.* (Accepted 2008).
15. E. Pelicon, J. H. Rohling, A. N. Medina, A. C. Bento, M. L. Baesso, D. F. de Souza, S. L. Oliveira, J. A. Sampaio, S. M. Lima, L. A. O. Nunes, T. Catunda, "Temperature dependence of fluorescence quantum efficiency of optical glasses determined by thermal lens spectrometry," *J. Non-Cryst. Solids*, **304**, 244-250 (2002).

1. Introduction

Based on tightly focused laser beams, photothermal (PT) techniques have been widely used as highly sensitive tools to determine optical and thermal properties of various materials [1-6]. The basic principle of the photothermal techniques is the photo-induced heat generation by non-radiative decay process following optical energy absorption of a sample, and the heat can cause a number of different effects, which provide various detection mechanisms. The information of the temperature rise in the sample as well as its thermophysical parameters can be obtained with these detection methods. For instance, when a focused excitation TEM_{00} laser beam impinges on a solid sample, a local thermal expansion and then a surface displacement are produced. This surface deformation depends on the optical, thermophysical properties of the sample and acts as a concave or convex mirror to a second TEM_{00} laser shining on the deformed surface [6,7]. This phenomenon is called thermal mirror (TM) effect. Recently [8,9], we have theoretically and experimentally demonstrated the useful and practical applications of the TM effect to measure absolute values of thermophysical properties of solids using a Gaussian excitation laser.

Although the PT techniques have been applied to the research in a variety of areas, the high cost of a TEM_{00} Gaussian laser (usually a high power gas laser) as an excitation light source limits potential applications. In order to expand the applicability of photothermal techniques, it is desirable to use less expensive non-Gaussian excitation laser to replace the Gaussian one. Li and co-workers [7,10] introduced a non-Gaussian laser beam with a top-hat intensity profile (top-hat excitation) into the PT techniques. They developed a theoretical model for modulated cw laser thermal lens (TL) optimized for a near field detection. They theoretically showed that with the optimum geometry its sensitivity would be twice higher than the Gaussian excitation one. In other attempts, Li et al used pulsed surface thermal lens and pulsed photothermal deflection techniques to qualitatively determine thermoelastic and the thermo-optical responses of ultraviolet dielectric coatings and nonlinear absorption coefficient of bulk materials, respectively [7,10]. However, a theoretical model, with which physical properties can be quantitatively determined, is necessary for practicable applications of PT spectroscopies with the top-hat laser excitation. Recently we reported a theory and quantitative measurement of time-resolved mode-mismatched TL spectroscopy induced by a cw top-hat excitation [11]. The analytical equation for the TL signal was used to fit the experimental data, and thermo-physical properties of the glass samples were quantitatively determined.

Considering the practical significance of the photothermal techniques for material characterization with less expensive excitation lasers, in this work, we derive a theory for the time-resolved TM of low absorbing samples using a cw top-hat excitation. Fitting to the theory, we quantitatively deduce the optical and thermal properties of glass samples, well consistent with the literature values. Moreover, using a cw top-hat excitation, we develop a time-resolved mode-mismatched experimental apparatus, which can be used for either a single TM measurement or a single TL measurement. For optically transparent samples, concurrent TM and TL measurements also can be performed using the apparatus. Experimental results show that the concurrent measurements can get more information on the physical properties of a sample than that obtained by a single TM or TL measurement.

2. Theory

The TM geometry used for the theoretical analyses is shown in Fig. 1(a). The theoretical analysis involves the calculations of (1) temperature rise in the sample, (2) the thermoelastic deformation on the sample surface due to the temperature rise, (3) the electric field phase shift of the probe beam reflected from the deformation, and (4) the intensity of the probe beam at the detector plane.

2.1. Temperature field produced by the cw top-hat laser beam excitation

The sample is treated as a radially infinite medium [3-5,8-9,14]. Heat flow along the beam axis in the low absorption sample is ignored, and only radial heat flow is considered [8,14]. As described in [11], the top-hat source profile follows a Unit-step function $\mathbf{U}(x)$ as

$$Q(r) = \frac{P_e A_e \phi}{\rho c \pi \omega_{0e}^2} \mathbf{U}(\omega_{0e} - r), \quad (1)$$

in which P_e is the excitation beam power, A_e the optical absorption coefficient of the sample at the excitation beam wavelength, and $\phi = 1 - \eta \lambda_e / \langle \lambda_{em} \rangle$. λ_e is the excitation beam wavelength, $\langle \lambda_{em} \rangle$ the average wavelength of the fluorescence emission, and η is the fluorescence quantum efficiency, which competes for a share of absorbed excitation energy. The solution of the heat transfer equation $c \rho \partial T(r, z, t) / \partial t - k \nabla^2 T(r, z, t) = Q(r)$ [12], with the initial condition $T(r, z, 0) = 0$ and the boundary conditions $T(\infty, z, t) = 0$ and $\partial T(r, z, t) / \partial z|_{z=0} = 0$, is given by [11]

$$T(r, z, t) = 4T_0 \int_0^\infty \left(\frac{1 - e^{-\alpha^2 \omega_{0e}^2 / 4t_c}}{\alpha^2 \omega_{0e}} \right) J_0(r\alpha) J_1(\omega_{0e} \alpha) d\alpha, \quad (2)$$

in which $J_n(x)$ is the n-order Bessel function of the first kind. c , ρ and k are the specific heat, mass density, and thermal conductivity of the sample, respectively. $t_c = \omega_{0e}^2 / 4D$ is the characteristic thermal time constant, and $D = k / \rho c$ is the thermal diffusivity of the sample, and $T_0 = P_e A_e \phi / 4\pi k$.

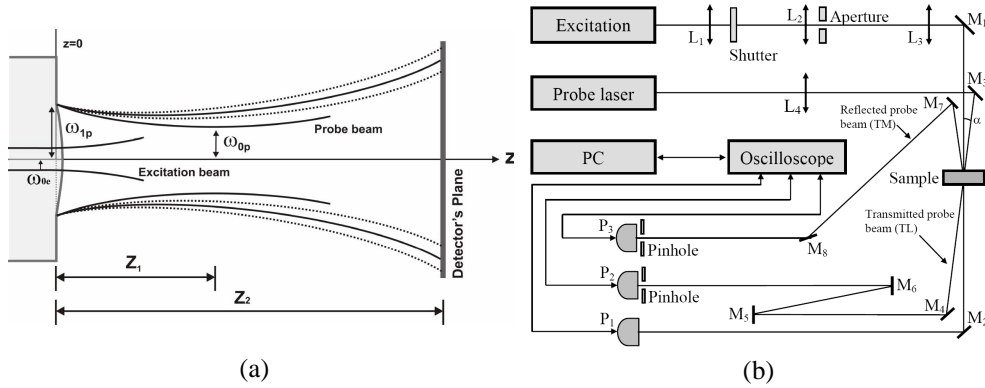


Fig. 1. (a) A scheme of the geometric arrangement of the beams in a mode-mismatched dual-beam TM experiment. ω_{0e} and ω_{0p} are the radii of the excitation and probe beams in the sample, respectively. ω_{0p} is the probe beam waist at the distance Z_1 from the sample, and Z_2 is the distance between the sample and the TM detector plane. (b) A schematic diagram of a time-resolved experimental apparatus for concurrent measurements of the TM and TL with top-hat cw laser excitation. Mi, Li, and Pi stand for mirrors, lenses and photodiodes, respectively. We used $\omega_{0p} = 920 \mu\text{m}$, $Z_1 = 275 \text{mm}$, $Z_c = 18 \text{mm}$, $V = 15.2$, $\omega_{0e} = 255 \mu\text{m}$, $m = 13$, and $Z_2 = 5 \text{m}$.

2.2. Surface deformation

In the quasi-static approximation, the surface thermoelastic deformation caused by a laser-induced non-uniform temperature distribution is given by [10,13,14]

$$(1 - 2\nu) \nabla^2 \mathbf{u} + \nabla(\nabla \cdot \mathbf{u}) = 2(1 + \nu) \alpha_T \nabla T(r, z, t), \quad (3)$$

and the boundary conditions at the free surface are $\sigma_{rz}|_{z=0} = 0$ and $\sigma_{zz}|_{z=0} = 0$ [13]. Here \mathbf{u} is the displacement vector; α_T is the linear thermal expansion coefficient. ν is the Poisson's ratio, and σ_{rz} and σ_{zz} are the normal stress components.

The solution of Eq. (3) can be expressed, in cylindrical coordinates due to the geometry of top-hat excitation laser beam, by introducing the scalar displacement potential ψ and the Love function Ψ [13]. By using the temperature rise distribution, Eq. (2), and the boundary condition over the stress [8,9,14], the z component of the displacement vector at the sample surface ($z = 0$), $u_z(r, 0, t)$, takes the form

$$u_z(r, 0, t) = -(1 + \nu)\alpha_T T_0 \int_0^\infty \alpha^2 f(\alpha, t) J_0(r\alpha) d\alpha, \quad (4)$$

with

$$f(\alpha, t) = (4/\alpha^5 \omega_{0e}) \left[1 - \exp\left(-\frac{t\alpha^2 \omega_{0e}^2}{4t_c}\right) \right] J_1(\alpha \omega_{0e}). \quad (5)$$

2.3. Probe beam phase shift

The surface deformed acts as an optical element, causing a phase shift $\Phi_{TM}(r, t) = 4\pi u_z(r, 0, t)/\lambda_p$ [8] to the reflected probe beam. λ_p is the probe beam wavelength. Using (4) and (5), the induced TM phase shift is

$$\Phi_{TM}(g, t) = \theta_{TM} \int_0^\infty \alpha^2 f(\alpha, t) J_0(\sqrt{mg} \omega_{0e} \alpha) d\alpha, \quad (6)$$

with $g = (r/\omega_{1p})^2$. $m = \omega_{1p}^2 / \omega_{0e}^2$ provides the degree of the mode-mismatching of the probe beam and excitation beam, and θ_{TM} is given by

$$\theta_{TM} = -\frac{2P_e A_e \alpha_T (1 + \nu) \phi}{\lambda_p k}. \quad (7)$$

The phase shift Φ_{TM} describes the distortion of the wavefront of the probe beam caused by the temperature-induced surface displacement of the sample.

2.4. Probe beam intensity at the detector plane

The complex electric field of the reflected probe beam, which is subject to a phase shift Φ_{TM} , is given by

$$U(r, Z_1) = B \exp\left[-i\left(\frac{\pi}{\lambda_p} \frac{r^2}{R_{1p}} + \Phi_{TM}\right) - \frac{r^2}{\omega_{1p}^2}\right]. \quad (8)$$

Here, B is a constant [8]. The propagation of the reflected probe beam to the detector plane can be treated as diffraction using Fresnel diffraction theory [5]. Considering only the centre of the probe beam spot at the detector plane, its complex amplitude can be written as $U(Z_1 + Z_2, t) = C \int_0^\infty \exp[-(1 + iV)g - i\Phi_{TM}(g, t)] dg$ [5]. C is a constant [5].

The intensity of the probe beam at the detector plane $I(t)$ then can be calculated as $I(t) = |U(Z_1 + Z_2, t)|^2$. Here the absorbed power of the probe beam by the sample is assumed

to be negligible compared with that of the excitation beam and has no contribution to the generation of the TM effect. The foregoing theoretical model was experimentally validated.

3. Experimental results

In this work an experimental apparatus for the measurement of either the TM or TL was developed, as shown in Fig. 1(b), which also could be used for the concurrent measurements of the TM and TL. A multi-mode diode-pumped solid-state laser (Melles Griot, Model 85 GLS 309, 532.0 nm) acted as an excitation laser. The top-hat intensity profile on the sample was created using a set of lenses (L_1 and L_2), a pupil, and a lens (L_3) in the same way as described in Reference [11]. A weak TEM₀₀ Gaussian He-Ne laser at 632.8 nm (Melles Griot, Model 05LHP151), focused by lens L_4 ($f = 20$ cm) and almost collinear to the excitation beam ($\alpha < 1.5^\circ$), was employed as a probe beam. A low absorption sample was positioned near the confocal plane of the probe beam. The exposure of the sample to the top-hat excitation laser was controlled by a shutter (ThorLabs, Model SH05), creating a TM on the sample surface and a TL in the sample. The reflected part of the probe beam from the TM was intercepted by a pinhole-photodiode (P_3) assembly, thus sensing the TM signal. The transmitted part of the probe beam through the TL was captured by another pinhole-photodiode (P_2) assembly to detect the TL signal. The signals from P_2 and P_3 were sent to a digital oscilloscope (Tektronics, Model TDS 3052), which was triggered by a photodiode P_1 , to record the signals. The experimental parameters are shown in the caption of Fig. 1, which were measured as described in Reference [11]. A computer was used to control the experimental apparatus and measurements.

The concurrent TM and TL measurements were performed with three well-known low absorption glass samples to test the theoretical model. These samples were: 0.1wt% CoF₂ doped ZBLAN glass [16], 2wt% Fe₂O₃ doped Soda lime glass [5], and 2wt% Nd₂O₃ doped low silica calcium aluminosilicate glass (LSCAS-2) [8,15].

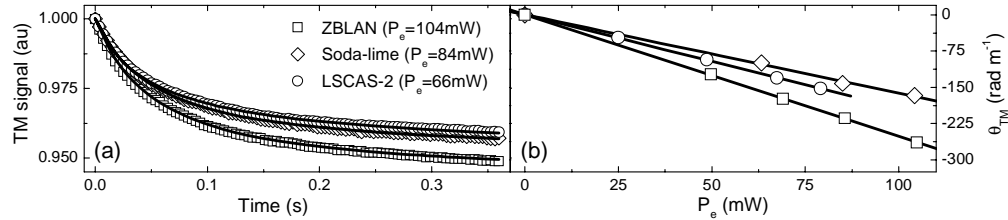


Fig. 2. (a). Normalized TM signals $I(t)/I(0)$ for the glass samples. (b) The fitted θ_{TM} as a function of excitation power for TM experiments. Open dots are experimental data and solid lines are best curve fitting.

Figure 2(a) shows examples of normalized transients of the TM signals of the glasses. The positive thermal expansion coefficients for all three glasses govern the shape of the TM transients. In this case, the produced surface deformations act as convex mirrors, defocusing the probe beam reflected from the TM and hence decreasing the signal at the detector. The numerical curve fitting of the transients to the theoretical model, corresponding to the solid lines in Fig. 2(a), deduced the values of t_c that is related to the thermal diffusivity and θ_{TM} . The thermal diffusivities of these glasses measured using the TM, shown in the Table 1, are consistent with previously measured using TL technique [11] and are also in good agreement with the literature values [5,15,16]. In the Table 1 are also listed the absorption coefficients A_e measured as described elsewhere [5] at the excitation wavelength. The linear dependences of the θ_{TM} on different excitation power were also obtained with the curve fitting for the glasses, as shown in Fig. 2(b). Table 1 shows the values of the slopes $d\theta_{TM}/dP_e$ of the glasses.

In addition to the D and θ_{TM} , θ_{TL} is also deduced from TL measurements [11]. Referring to Eq. (7) for θ_{TM} and to Eq. (4) in Ref. [11] for $\theta_{TL} = -P_e A_e l(ds/dT)\phi/\lambda_p k$, the phase shifts

of both the TM and TL are associated with the thermal conductivity k , optical absorption coefficient A_e , and fluorescence quantum efficiency η . Also, θ_{TM} is dependent on the thermo-mechanical properties, namely linear thermal expansion coefficient α_T and the Poisson's ratio ν . For a fluorescent sample, the TM can be used to determine the η with no requirement of a reference sample, providing the α_T and ν are known. Using the listed parameters in the Tables 1 plus $\langle\lambda_{em}\rangle=1064$ nm [15] for the LSCAS-2, we found $\eta = 0.84$, consistent with the literature value [15] measured with a reference.

Besides the k , A_e , and η , the thermal lens phase shift θ_{TL} [11] is also related to the temperature coefficient of the optical path length ds/dT , an important thermo-optical parameter of optical materials, such as a solid state laser material, correlated to light wavefront distortion induced by a temperature variation [14,16]. For a fluorescent sample, it is usually difficult to determine the ds/dT and η simultaneously using the TL. Combining the θ_{TL} and θ_{TM} , one can calculate the ds/dT with $ds/dT = 2\alpha_T(1+\nu)\theta_{TL}/(\theta_{TM}l)$ without the knowledge of the k , A_e , and η . Thus, the combination of the TL and TM with the same top-hat excitation and Gaussian probe lasers provides a novel approach to measure the ds/dT . The TL results obtained in this work are, as expected, the same as that obtained previously [11]. Using the measured TL and TM results, we determined ds/dT for the three samples (Table 1). These values are in good agreement with the literature data for these materials [5,15,16]. Moreover, for non-fluorescent samples of weak absorption or scattering, sometimes the measurement of A_e introduces an experimental error, and this approach can reduce the error in the determination of the ds/dT . Alternatively, this approach can be employed to quantify the mechanical property if the ds/dT is known.

Table 1. The results of the TM experimental measurements

Samples	A_e (Measured) (cm^{-1})	D (Measured) ($10^{-3} \text{ cm}^2/\text{s}$)	$d\theta_{TM}/dP_e$ (Measured) ($10^3 \text{ W}^{-1}\text{m}^{-1}$)	ν (Literature)	α_T (Literature) (10^{-6} K^{-1})	k (Literature) (W/mK)	ds/dT (Measured) (K^{-1})
LSCAS-2 [15]	1.70±0.03	5.9±0.3	-(1.94±0.04)	0.29	7.5	1.50	12.1±0.5
ZBLAN [16]	0.35±0.01	3.1±0.3	-(2.51±0.05)	0.25	14.0	0.77	-(5.8±0.3)
Soda-lime [5]	1.00±0.03	5.1±0.3	-(1.62±0.06)	0.21	5.2	1.20	5.2±0.3

4. Conclusion

A theoretical model for time-resolved TM of low optical absorption samples induced by a top-hat cw laser excitation was developed. An experimental apparatus for concurrent measurements of the TM and TL was developed with a top-hat excitation laser. Three low absorption glass samples were tested, and their thermophysical properties were quantitatively determined with the theory and apparatus and found to be consistent with the literature values, indicating the theory is practicable. Furthermore, η and ds/dT could be determined simultaneously without any reference by using the combined results of the TL and TM measurements, showing the usefulness of the concurrent measurement. The theoretical model and experimental apparatus developed in this work make it promising to use a top-hat laser excitation in the TM and TL measurements, thus expanding the applicability of photothermal techniques with a less expansive non-Gaussian excitation laser.